

MAGNETIC-FIELD COMPRESSION BY SHOCK-INDUCED CONDUCTION WAVES IN HIGH-POROSITY MATERIALS

E. I. Bichenkov, S. D. Gilev,
A. M. Ryabchun, and A. M. Trubachev

UDC 539.63; 537.311.3

Introduction. The method of magnetic-flux compression by shock waves of closed configuration converging to a certain axis and transforming the nonconducting material to a conducting state was independently proposed by the authors of this paper [1–3] and K. Nagayama et al. [4, 5]. The method differs from classical magnetic cumulation by the loss of a great portion of magnetic flux that is “trapped” into the conducting material formed behind the shock-wave front. This limits crucially the energy potentials of the method. However, despite the significant flux losses in the compression region, the compression of a magnetic field together with the material offers a number of advantages. These advantages are associated with current generation in a fresh conducting material and with the possibility of using the hydrodynamic-cumulation effect to increase the mechanical-energy density and, hence, its related density of magnetic-field energy. Using the shock-wave method, megagauss magnetic fields were generated in low-cost generators of extremely simple design [6, 7]. The highest registered field was 3.5 MGs with a magnetic field amplification factor $\beta = B/B_0 \sim 90$ [8].

The general energy estimates of [6] for the simplest model of a material packed to a constant density have shown that the possibilities of the method depend fundamentally on the packing parameter of the material $n = \rho/\rho_0$. It was found that, in sufficiently rigid materials with packing $n \leq 2$, retardation of a magnetic field by a shock wave does not lead to a marked loss of energy by the wave, the magnetic energy in the compression region does not increase, and the case of complete closure of shock waves does not contradict the law of energy conservation. In this case, the magnetic energy remains finite, and the magnetic flux completely enters the conductor, while the magnetic-flux density tends theoretically to increase strongly with a limited initial energy of the system. The estimates presented in [6] show that when the material behind the shock-wave front is incompressible, the maximum magnetic field is determined by the conductance and geometrical dimensions of the generator, which enter into the expression for the limiting field in the combination corresponding to the magnetic Reynolds number Re_m , i.e., as in classical magnetic cumulation, the restriction of shock-wave compression possibilities by the finite electrical conductivity of the material appears to be of no principal importance: an increase in the dimensions of the system can ensure high values of Re_m , and one can expect the corresponding increase in the generated magnetic field.

Among the studied materials, the maximum fields and the highest amplification of the magnetic field were obtained in heterogeneous materials such as an aluminum powder with an initial density of the order of 0.1–0.2 of the monolithic density. Since shock compression of highly porous materials is accompanied by strong heating, one can expect that magnetic compression in these materials occurs with a significant loss of energy to the material filling the MC generator, and precisely this factor limits the values of attainable magnetic fields. The object of this study was to determine the effect of compressibility of high-porosity materials on magnetic cumulation in shock-induced conduction waves.

K. Nagayama [9] and A. A. Barmin et al. [10] attempted to take into account the properties of shock-compacted materials. Their results agree to a certain degree with experimental data. Nagayama calculated

Lavrent'ev Institute of Hydrodynamics, Siberian Division, Russian Academy of Sciences, Novosibirsk 630090. Translated from *Prikladnaya Mekhanika i Tekhnicheskaya Fizika*, Vol. 37, No. 6, pp. 15–25, November–December, 1996. Original article submitted August 30, 1995.

the field compression in metal powders using the Mie–Grüneisen approximation. Barmin et al. analyzed CsI and used approximations for pressure and internal-energy data as the functions of temperature and specific volume obtained on the basis of free-volume theory in the Lennard-Jones interpretation. In some calculations, they used the model equation of state based on the assumption that the ratios of pressure to density and to temperature remain constant in the particle behind the shock-wave front and represented the pressure and temperature on the Hugoniot adiabat by power functions of density fitted to empirical data.

In the present paper, we used another approach to choose the equation of state for a shock-compressed material. Considerable attention is given to the search for an approximation that would describe satisfactorily the behavior of high-porosity materials over a wide range of variation of the initial density. The calculations yielded new qualitative features of field and material compression that were not found in [9, 10].

This paper reports numerical results for compression of a magnetic flux by a cylindrical shock wave converging to the axis and transforming the nonconducting material to a conducting state. The calculations were performed for various metal powders with a low initial density. We studied the dependence of the highest magnetic field attainable at the compression stage on the type of material, initial density of material, and initial magnetic field for fixed parameters of a shock-generating unit. For some materials and in a rather narrow range of initial fields, velocity oscillations of the convergent wave were found. The material-flow structure was analyzed in detail. The oscillations are shown to result from the superposition of energy cumulation in the compacted material on hydrodynamic and magnetic cumulation.

The calculations have shown that a great portion of the energy is taken by the material, i.e., the compressibility of materials is the major factor that limits achievable magnetic fields, as is the case for classical magnetic cumulation.

Equation of State for Highly Porous Materials. Selection of an equation of state is the most important point in solving the problem of shock compaction. At the present time, experimental data on the state of condensed materials at high pressures has been obtained predominantly by shock-wave methods for a vast variety of materials [11]. It is conventional to represent the shock adiabat of solid materials as a linear relation between the wave and mass velocities:

$$D = a + bu. \quad (1)$$

Shock-wave relations make it possible to obtain the pressure p , specific volume $V = 1/\rho$, and internal energy ε from (1). That is, one obtains a certain line of states in the space of the three thermodynamic parameters that lies on the surface $\varepsilon = \varepsilon(p, V)$, which is an equation of state. It is obvious that knowledge of the material's shock adiabat does not give the entire surface of possible states of the material. Therefore, in deriving the equation of state, the Hugoniot adiabat is used only as a supporting line from which extrapolation is performed by one or another rule and, thus, an approximate form of a certain range on the surface of states is determined in the vicinity of the shock adiabat.

At present, the most widely used extrapolation is likely the Mie–Grüneisen extrapolation

$$\Delta E = \frac{V}{\gamma} \Delta p, \quad (2)$$

in which the Grüneisen coefficient γ is primarily determined empirically. Use of the Mie–Grüneisen relation for high-porosity materials involves some difficulties, because, under compression, pressure varies over a very wide range, and the only fixed parameter γ is insufficient. For such materials it is appropriate to extrapolate from the shock adiabat with respect to specific volume [instead of pressure, as in (2)], since its variation under shock compression is always limited and fairly small, especially for condensed materials. Such a procedure for deriving the equation of state was proposed by Oh and Person [12] as the relation

$$\left(\frac{\partial E}{\partial V}\right)_H = -\left(\frac{\partial E}{\partial V}\right)_p, \quad (3)$$

in which the derivatives of internal energy with respect to specific volume on the shock adiabat and on the isobar are assumed to be equal in magnitude and opposite in sign. Relation (3) is nontrivial and is not well founded. In the simplest case, it can be written as finite differences, and this allows the surface of possible states

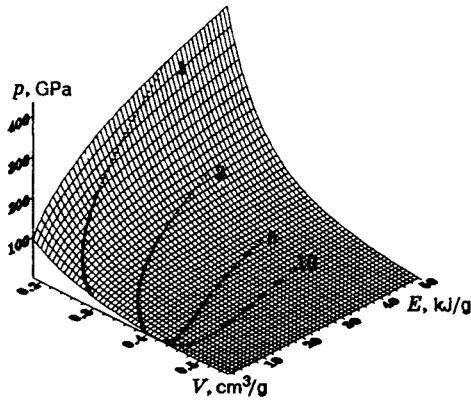


Fig. 1

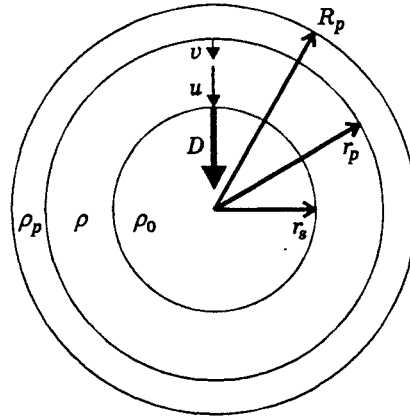


Fig. 2

TABLE 1

Material	$\rho_0, \text{g/cm}^3$	$a, \text{km/sec}$	b	Material	$\rho_0, \text{g/cm}^3$	$a, \text{km/sec}$	b
Al	2.71	5.333	1.356	Cu	8.90	3.900	1.733
Be	1.84	7.993	1.132	Ti	4.5	5.22	0.767

of a solid material in the space $\{p, V, \varepsilon\}$ to be obtained from the shock-compression curve of the material by a very simple procedure. A thorough testing showed that, besides being very simple, the Oh–Person equation describes well the behavior of shock-compressed materials over wide ranges of porosity and explosive-loading intensity, and, for highly porous materials, it is preferred to the Mie–Grüneisen relation.

The thus-calculated surface of states for aluminum is shown in Fig. 1. The porosity values are shown near the curves corresponding to shock adiabats. The porosity values were determined as the ratio of monolithic density to the initial density of the material. Thus, 1 corresponds to the solid material, and 10 corresponds to the material whose density is 0.1 of the density of the solid material. Note that the shock adiabats clearly show the abnormal run of the specific-volume–pressure curves in the region of moderate pressures (a higher pressure leads to a lesser compaction of the materials) [13].

The limitations of the method of deriving the equation of state proposed by Oh and Person are due to the impossibility of describing phase transitions and chemical transformations when new components with new shock-adiabat parameters arise. Therefore, use of the above extrapolation is restricted to materials with sufficiently high energy thresholds of phase transformations or to materials for which the energy of phase transformation is low and the difference between shock-wave properties in different phases is insignificant. It is therefore believed that, despite the possibility of melting of high-porosity specimens under compression, this approximation is acceptable for metals, since the shock-wave parameters of metals change only slightly upon melting and the heat of melting is relatively small.

In the present paper, condition (3) was used as a separate calculation subprogram of the equation of state in the form $\varepsilon = \varepsilon(p, V)$. The constants of shock adiabats of solid materials used in the calculations are listed in Table 1 (the data are taken from [11]).

System of Equations and Formulation of the Problem. We consider magnetic-field compression by a convergent cylindrical wave produced by impact of a liner with a given weight at a prescribed initial velocity on a cylindrical sphere which is coaxial with the liner (Fig. 2). In Fig. 2 and below, the subscript p is used to describe the state and motion of the liner (piston), the subscript s is used for the shock wave, and the subscript 0 for initial parameter values.

We analyzed the following two cases: complete filling of the compression region by the material, and incomplete filling in which the material was concentrated at the center of a cylindrical cavity with radius

$r_0 = 0.4r_{p0}$. This scheme of magnetic compression is called hybrid, since classical magnetic cumulation occurs in the first stage, and, after collision of the liner with the material, shock-wave squeezing of the magnetic flux takes place. The material was initially nonconducting. Upon passage of a shock wave, it acquires a considerable conductivity, which allows one to assume that the magnetic field behind the shock front is "trapped" into the material.

In our calculations, we used Lagrangian coordinates. The mass variable s was determined for an angle of 1 rad, so that $\partial s/\partial(r^2) = -\rho/2$. The trapped-field condition leads to $B(s) = \Phi(s)\rho(s)$, where $\Phi(s)$ is the magnetic flux related to the unit mass of the material. The total pressure in the material is $p_m(s) = p(\varepsilon, \rho) + \Phi^2(s)\rho^2(s)/2\mu_0$.

The problem is described by the following system of equations of magnetic hydrodynamics [14]:

$$\frac{\partial}{\partial t} \left(\frac{1}{\rho} \right) = \frac{\partial(ur)}{\partial s}, \quad \frac{\partial r}{\partial t} = u, \quad \frac{\partial u}{\partial t} = -r \frac{\partial p_m}{\partial s}, \quad \frac{\partial \varepsilon}{\partial t} = -p \frac{\partial(ur)}{\partial s}.$$

Boundary conditions were formulated on the material–liner interface and on the shock wave. Assuming that the liner material is incompressible with density ρ_p and the pressure on its outer surface is equal to zero, and ignoring magnetic-field diffusion to the thin skin-layer formed on the inner surface of the liner, one can easily obtain the following equation of motion for the liner from the Euler equation:

$$\frac{dv}{dt} = -\frac{v^2}{r_p \ln(1 - m_p)} \left(m_p + \ln(1 - m_p) + \frac{2p_m(0, t)}{\rho_p v^2} \right), \quad m_p = \frac{m}{m + \pi \rho_p r_p^2}.$$

Here r_p is the location of the inner surface of the liner, m is the liner mass per unit length along the axis, m_p is the mass coefficient for the liner, and p_m and v are the total pressure on the inner surface of the liner and the velocity of the surface. The Lagrangian coordinate $s_p = 0$ corresponds to this surface.

The following conditions are satisfied at the shock front $s = s_s(t)$:

$$\rho(s_s) = \frac{\rho_0 D(s_s)}{D(s_s) - u(s_s)}; \quad (4)$$

$$p(s_s) = \rho_0 D(s_s) u(s_s); \quad (5)$$

$$\frac{dB}{dt} = B \frac{2u(s_s)}{D(s_s)}; \quad (6)$$

$$\frac{ds_s}{dt} = -\rho_0 r_s D(s_s); \quad (7)$$

$$\varepsilon(s_s) = \frac{u^2(s_s)}{2}. \quad (8)$$

The first two conditions are the well-known continuity and momentum equations. Relation (6) is the equation of magnetic-flux compression with allowance for entrapment of the field into the conductor formed behind the shock wave and the related removal of a portion of the magnetic flux from the compression region. This relation was derived in [6, 7]. Condition (7) follows from the definition of the Lagrangian coordinate. The equality of the kinetic energy of the material to the change in its internal energy (8) is valid if the pressure behind the shock front is much higher than the initial pressure in the material. For the compression of porous materials, this assumption is conventional [13].

The initial conditions for the moment of collision of the liner with the materials for $s_{s0} = s_{p0} = 0$ have the form

$$r_s = r_0, \quad u = v_0, \quad B = B_0, \quad \varepsilon = \frac{v_0^2}{2}, \quad p_m(s_{s0}) = \rho_0 D(v_0) v_0 + \frac{B_0^2}{2\mu_0}, \quad \rho(s_{s0}) = \frac{\rho_0 D(v_0)}{D(v_0) - v_0}.$$

In the hybrid scheme, the velocities of the liner and the magnetic field at the beginning of the shock-wave compression phase were recalculated under the assumption of an ideal character of the first stage of flux compression.

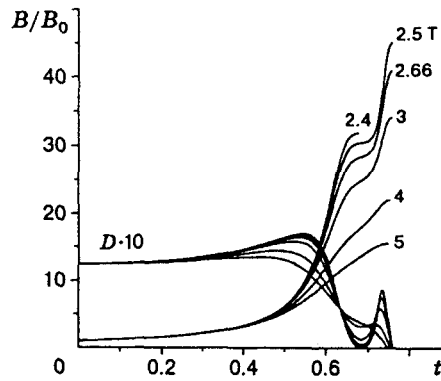


Fig. 3

The thus-formulated problem was solved numerically for various materials with different initial porosities and initial fields. Since experimental variations in the liner size, material, and velocity are labor-consuming and expensive, the shock-unit parameters were assumed fixed. In our calculations, the initial conditions for the liner were as follows: mass $m = 102 \text{ g/cm}$, density of material $r_p = 8.92 \text{ g/cm}^3$, velocity $v_0 = 2000 \text{ m/sec}$, and diameter $r_{p0} = 7.5 \text{ cm}$. In the introduction of dimensionless variables, all dimensions were referred to the initial radius r_0 of the core filled with the material, the velocities were referred to the shock-wave velocity D_0 at the moment of impact of the liner on the material, the times to r_0/D_0 , and the magnetic field to the characteristic field $B_0 = \sqrt{2\mu_0 T_0 / \pi r_0^2}$ determined from the initial kinetic energy T_0 of the liner.

For incomplete filling of the compression region, the initial density of the material was considered constant and equal to 0.44 g/cm^3 for aluminum powder. When the compression cavity was completely filled, the initial density was varied to study some unexpected features of magnetic compression in shock-induced conduction waves that were found in a series of calculations for hybrid MC generators.

Calculation Results. In all calculations, we excluded the possibility of return motion of the wave front, since there are no grounds to assume that in this case the shock wave will not be destroyed by instabilities at the field-substance interface. Thus, it was assumed that the shock wave was decelerated by the magnetic pressure as long as the wave was capable of producing a fresh conducting material behind itself. In the program, the calculation was terminated when the shock-front velocity vanished.

The occurrence of shock-front-velocity oscillations for certain values of the initial field and for a certain degree of filling of the compression cavity by the material is likely the most interesting fact revealed in the calculations. This phenomenon is illustrated in Fig. 3. The time dependences of the field-amplification coefficient B/B_0 and the wave velocity D for the hybrid compression scheme in porous aluminum are shown in a combined graph. The calculations have shown that the final field increases strongly with a decrease in the initial field. The shock velocity first tends to increase, but as the magnetic field reaches higher values the shock velocity decreases sharply, passes through a minimum, increases again, and, finally, decreases sharply to zero. In the region of minimum wave velocity, the field is stabilized at a certain value; a ledge appears in the graph.

A large number of calculation results for hybrid MC generators with aluminum and titanium as working materials are presented in Fig. 4. One can see that wave-velocity oscillations occur in a narrow range of initial fields and depend greatly on the material. For titanium, this is a hardly noticeable ledge in the region of positive velocities, and, for copper, oscillations in this region are not observed. The calculation results for beryllium are close to those for aluminum. For shock generators with a completely filled cavity and a fixed shock unit, velocity oscillations are observed when the material mass remains the same as in the hybrid scheme, i.e., the density of the material should be inversely proportional to the fullness of the compression cavity.

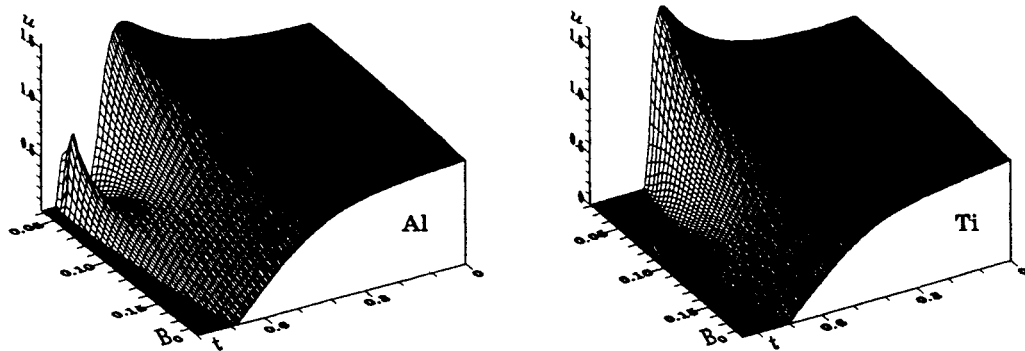


Fig. 4

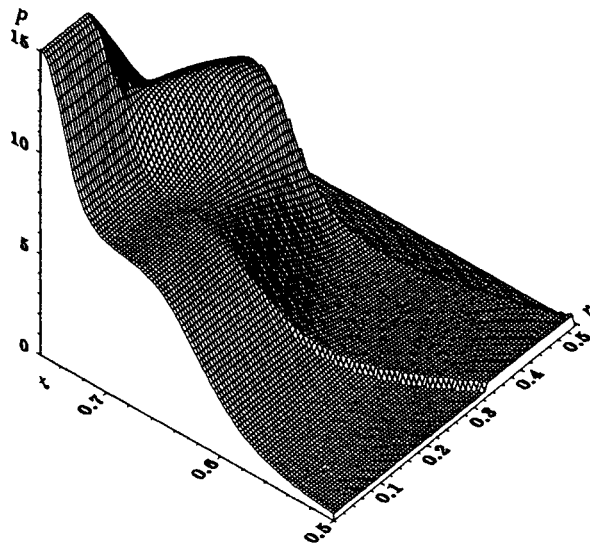


Fig. 5

The details of the material flow in the region of wave-velocity oscillations could be understood from an analysis of the pressure, mass-velocity, and material-flow distributions in the final compression stages (shown in Figs. 5-7) in which the wave-velocity oscillations manifested themselves. It is evident from the graphs that when compression begins, the magnetic pressure is low but increases monotonically with time, and the pressure jump at the shock front is almost constant in magnitude and is clearly seen against the background of the magnetic component of pressure. Behind the jump, the total (magnetic and hydrodynamic) pressure is at first almost constant, but with time it shows a tendency to decrease in moving from the shock wave into the material. This is associated with the distribution of the magnetic field trapped into the material and the total-pressure component produced by the magnetic field.

At the compression stage near the velocity minimum, the magnetic field reaches a considerable value and begins to affect markedly the motion of the material. As a result, the shock-wave velocity decreases, the magnetic field is stabilized, and the pressure jump at the shock front decreases and becomes almost unobservable against the background of the high magnetic pressure. Deep in the compressed material, the motion to the axis continues. As a result, a high-pressure region forms which causes the material to decelerate on the periphery and to accelerate in the near-axis zone. Thus, redistribution of the kinetic energy in the material occurs. For incompressible fluids, this phenomenon is known as hydrodynamic cumulation.

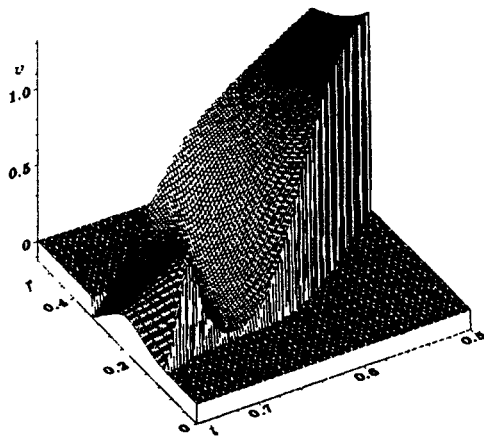


Fig. 6

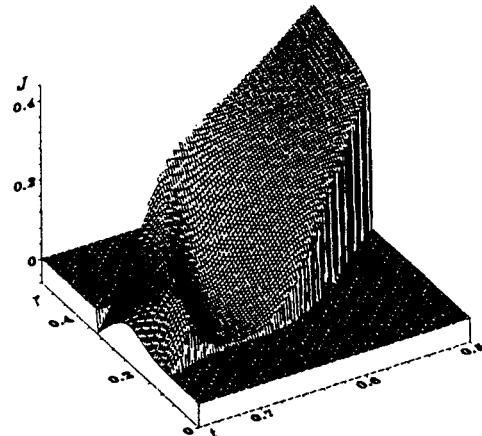


Fig. 7

The details of the mass-velocity distribution in the material are clearly seen in Fig. 6. It should be noted that the magnetic field decelerates primarily the inner layer of the material. The velocity head of the outer layers leads to energy redistribution in the material and attendant velocity oscillations at the shock front. In the final stages of motion, the material's velocity on the periphery is negative, since a part of the compressed material has reflected from its axis because of the high elasticity of the material.

To understand the dynamics of density variation, one should analyze the variation in the material flow (Fig. 7). Calculations have shown that, initially, the material is predominantly compressed. In the stage of shock-wave deceleration, this compression is very strong. After the passage of the velocity through the minimum, the compressed material begins to spread to the axis and in the opposite direction to form an outward directed flow in the peripheral zone.

The most nontrivial calculation result is that kinetic-energy cumulation occurs in a strongly compressible porous material. Sometimes, after packing the material can be sufficiently rigid for this effect to manifest itself. On the other hand, of importance is the material's compressibility, which should lead to accumulation of elastic energy that is great enough to accelerate again the material layer near the shock front that was decelerated by the magnetic field. We emphasize that the above features of motion and their relative manifestations depend greatly on the type of material and are observed in a relatively narrow range of values of the initial magnetic field. In principle, one can probably expect the occurrence of shock-front-velocity oscillations for any material. But the graphs in Fig. 4 show that these oscillations can be estimated only in the region of negative wave velocities. Taking into account the above-mentioned possibility of wave decay, we did not consider such solutions.

Interesting results were obtained in analysis of the energy balance at the moment the mass velocity vanished immediately behind the shock front. Tables 2 (incomplete filling) and 3 (complete filling) show calculation results for hybrid and shock-wave generators with aluminum as a working material. Here B_0 and B_f are the initial and final fields, T_f and A_p are the kinetic energy and the compression work at the moment the shock wave stops, referred to the initial source of mechanical and magnetic energy in the system, and ε is the sum of these two terms, which is the portion of energy lost for magnetic compression.

One can see that, for generator parameters producing the highest magnetic fields, the portion of energy lost in the material is great: approximately 1/2 for hybrid generators and 1/3 for shock-wave generators. The distribution of this energy between the kinetic energy and compression work of the material differs significantly, i.e., the kinetic energy is imperceptible in a hybrid generator, while it dominates in a shock-wave generator. The maximum field of hybrid generators is almost twice as high as that of shock-wave generators. In spite of the considerable difference between the maximum fields, the magnetic energy of shock-wave generators is greater by a factor of 1.5 than that of hybrid generators. This is the case because the area occupied by the

TABLE 2

B_0	B_f	T_f^*	A_p	ε
T				
2.66	683	94	0.44	0.45
3.00	641	77	0.41	0.42
4.00	549	28	0.33	0.33
5.00	484	4.3	0.25	0.25
6.00	432	0.14	0.19	0.19
7.00	389	0.033	0.14	0.14
8.00	352	0.004	0.10	0.10
9.00	320	0.000	0.07	0.07
10.00	293	0.000	0.05	0.05

TABLE 3

B_0	B_f	T_f	A_p	ε
T				
2.08	377	0.22	0.11	0.32
3.00	329	0.17	0.12	0.29
4.00	293	0.13	0.12	0.25
5.00	266	0.093	0.12	0.21
6.00	246	0.065	0.12	0.18
7.00	228	0.043	0.11	0.15
8.00	214	0.026	0.10	0.13
9.00	201	0.015	0.09	0.11
10.00	190	0.008	0.08	0.09

Note. The asterisk denotes that the values of T_f are multiplied by 10^4 .

strong field in a shock-wave generator is greater by a factor of 4. For high initial fields, the energy losses in materials are small in both cases and reduce mainly to the compression work. Again, the maximum field is much higher for a hybrid generator. Note also that the size of the area corresponding to the largest computed field is marked and equals $0.04r_0$ for the shock-wave compression scheme and $0.1r_0$ for the hybrid compression scheme.

Conclusion. The calculations have shown that the material's properties influence significantly the shock-wave compression of a magnetic flux, because a considerable portion of the liner energy is taken by the material. As in the case of classical magnetic cumulation, the energy capacity of the compressed material is most likely the major limitation of the possibilities of the shock-wave method of generating ultra-high magnetic fields. The nontrivial phenomenon of wave-velocity oscillations in the phase of convergence of a shock wave manifests itself in a relatively narrow range of values of the initial magnetic field and initial density of some materials. From a hydrodynamic viewpoint, the above features of shock-wave compression of a magnetic flux are an interesting superposition of hydrodynamic and magnetic cumulation in compressed materials.

Qualitative analysis of field compression in a material led Trubachev [15] to propose that the shock-wave velocity stabilizes when the shock wave is incident on the system axis. Our calculations have shown that this compression regime is not realized because of the limited sound velocity in a compressed material, i.e., the system is insufficiently rigid.

The results obtained in this work are consistent from a physical standpoint and are fairly intelligible, and this suggests the absence of errors in both the model used to describe the materials and the calculations. However, this indirect evidence is insufficiently reliable, because the extrapolation in the chosen equation of state is too strong. Unfortunately, carrying out necessary experiment is beyond the scope of the authors' possibilities at present. The authors are thankful to the International Science Foundation (Grant RBO000) and the Russian Foundation for Fundamental Research (Grant 94-02-04022) for their support.

REFERENCES

1. E. I. Bichenkov, N. G. Skorobogatykh, and A. M. Trubachev. USSR Inventor's Certificate No. 762706, Magnetocumulative Generator.
2. E. I. Bichenkov, S. D. Gilev, and A. M. Trubachev, "MC generators using the transition of a semiconductors to a conducting state," *Prikl. Mekh. Tekh. Fiz.*, No. 5, 125-129 (1980).
3. S. D. Gilev and A. M. Trubachev, "Shock-wave generation of high-power magnetic fields in materials," *Pis'ma Zh. Tekh. Fiz.*, 8, No. 15, 914-916 (1982).

4. K. Nagayama, "New method of magnetic flux compression by means of the propagation of shock-induced metallic transition in semiconductors," *Appl. Phys. Lett.*, **38**, No. 2, 109–116 (1981).
5. K. Nagayama, T. Oka, and T. Mashimo, "Experimental study of a new mechanism of magnetic flux cumulation by the propagation of shock-compressed conductive regions in silicon," *J. Appl. Phys.*, **53**, No. 4, 3029–3037 (1982).
6. E. I. Bichenkov, S. D. Gilev, and A. M. Trubachev, "Shock-wave MC-generators," in: V. M. Titov and G. A. Shvetsov (eds.), *Ultrahigh Magnetic Fields. Physics. Techniques. Applications*, Proc. 3rd Int. Conf. on Megagauss Magnetic Field Generation and Related Topics [in Russian], Nauka, Moscow (1984), pp. 88–93.
7. K. Nagayama and T. Mashimo, "Magnetohydrodynamic study of flux cumulation by the propagation of shock-compressed conductive regions in semiconductors," in: *ibid.*, pp. 270–277.
8. E. I. Bichenkov, S. D. Gilev, A. M. Ryabchun, and A. M. Trubachev, "Shock-wave method for generation of megagauss magnetic fields," in: *Megagauss Technology and Pulsed Power Applications*, Proc. of 4th Int. Conf. on Megagauss Magnetic Field Generation and Related Topics, Plenum Press, New York–London (1987), pp. 89–105.
9. K. Nagayama and T. Murakami, "Magnetohydrodynamic study of the interaction of magnetic flux with high-pressure shock waves in metal powder," in: *Shock Tubes and Waves*, Proc. of 16th Int. Symp. on Shock Tubes and Shock Waves, VCH, Aachen, W. Germany (1987), pp. 881–887.
10. A. A. Barmin, O. A. Mel'nik, A. B. Prichshepenko, et al., "Electromagnetic energy losses in compression of a magnetic field by a second-kind jump," *Izv. Akad. Nauk SSSR, Mekh. Zhidk. Gaza*, No. 6, 166–170 (1988).
11. L. V. Altshuler, A. A. Bakanova, I. P. Dudoladov, et al., "Shock adiabats of metals. New data, statistic analysis, and general laws," *Prikl. Mekh. Tekh. Fiz.*, No. 2, 3–34 (1981).
12. K. H. Oh and P. A. Person, "Equation of state for extrapolation of high-pressure shock Hugoniot data," *J. Appl. Phys.*, **65**, No. 10, 3352–3356 (1989).
13. Ya. B. Zel'dovich and Yu. P. Raizer, *Physics of Shock Waves and High-Temperature Hydrodynamic Phenomena* [in Russian], Nauka, Moscow (1966).
14. A. A. Samarskii and Yu. P. Popov, *Differential Methods of Solving Gas Dynamics Problems* [in Russian], Nauka, Moscow (1980).
15. A. M. Trubachev, "Shock-wave MC generators. Estimation of the limiting possibilities of the method," in: *Dynamics of Continuous Media* [in Russian], Institute of Hydrodynamics, Novosibirsk, **88** (1988), pp. 132–147.